

Review article based on an invited lecture given at the NATO Advanced Study Institute
 “The Neutron Star - Black Hole Connection” June 7-18 1999, Elounda, Crete.

RADIO PULSARS — AN OBSERVER’S PERSPECTIVE

D.R. LORIMER
National Astronomy and Ionospheric Center
Arecibo Observatory
HC3 Box 53995, Arecibo PR 00612, USA

Abstract. Pulsar astronomy is currently enjoying one of the most productive phases in its history. In this review, I outline some of the basic observational aspects and summarise some of the latest results of searches for pulsars in the disk of our Galaxy and its globular cluster system.

1. Preamble

Pulsar astronomy began serendipitously in 1967 when Jocelyn Bell and Antony Hewish discovered periodic signals originating from distinct parts of the sky via pen-chart recordings taken during an interplanetary scintillation survey of the radio sky at 81.5 MHz (Hewish et al. 1968). This remarkable phenomenon has since been unequivocally linked with the radiation produced by a rotating neutron star (Gold 1968, Pacini 1968). Baade & Zwicky (1934) were the first to hypothesise the existence of neutron stars as a stable configuration of degenerate neutrons formed from the collapsed remains of a massive star after it has exploded as a supernova.

Although the theory of pulsar emission is complex, the basic idea can be simply stated as follows: as a neutron star rotates, charged particles are accelerated out along its magnetic poles and emit electromagnetic radiation. The combination of rotation and the beaming of particles along the magnetic field lines means that a distant observer records a pulse of emission each time the magnetic axis crosses his/her line of sight, i.e. one pulse per stellar rotation. Like many things in life, the emission does not come for free. It takes place at the expense of the neutron star’s rotational kinetic energy — one of the key predictions of the Gold/Pacini theory.

Measurements of the secular increase in pulse period through pulsar timing techniques (§4) are in excellent agreement with this idea.

Pulsar astronomy has come a long way in a remarkably short space of time. Systematic surveys with the world’s largest radio telescopes over the last 30 years have revealed more than 1200 pulsars in a rich variety of astrophysical settings. The present “zoo” of objects is summarised in Fig. 1. Some of the highlights so far include: (1) The original *binary pulsar*

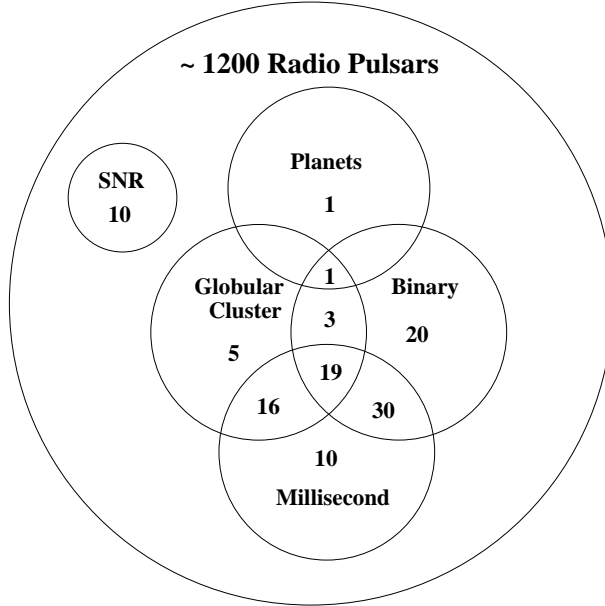


Figure 1. An adaptation of Dick Manchester’s Venn diagram showing the various types of radio pulsars. SNR denotes pulsars likely to be associated with supernova remnants.

B1913+16 (Hulse & Taylor 1975) — a pair of neutron stars in a 7.75-hr eccentric orbit. The measurement of the orbital decay due to gravitational radiation from the binary system resulted in the 1993 Physics Nobel Prize. (2) The original *millisecond pulsar*, B1937+21, discovered by Backer et al. (1982) has a period of only 1.5578 ms. The implied spin frequency of 642 Hz means that this neutron star is close to being torn apart by centrifugal forces. (3) Pulsars with planetary companions. Well before the discoveries of Jupiter-mass planets by optical astronomers, Wolszczan & Frail (1992) discovered the millisecond pulsar B1257+12 accompanied by three Earth-mass planets — the first planets discovered outside our Solar system. (4) Pulsars in globular clusters. Dense globular clusters are unique breeding grounds for exotic binary systems and millisecond pulsars. Discoveries of 40 or so “cluster pulsars” have permitted detailed studies of pulsar dynamics in the cluster potential, and of the cluster mass distribution.

The plan for the rest of this review is as follows: §2 covers pulse dispersion and what it tells us about pulsars and the interstellar medium; §3 discusses pulse profiles and their implications. In §4 the essential aspects of pulsar timing observations are reviewed. §5 reviews the techniques employed by pulsar searchers. Finally, in §6, we summarise some of the recent results from searches at Parkes. More complete discussions on the observational aspects covered here can be found in Lyne & Smith (1998).

2. Pulse Dispersion and the Interstellar Medium

Newcomers to pulsar astronomy would do well to begin their studies by reading the discovery paper (Hewish et al. 1968), a classic article packed with observational facts and their implications.

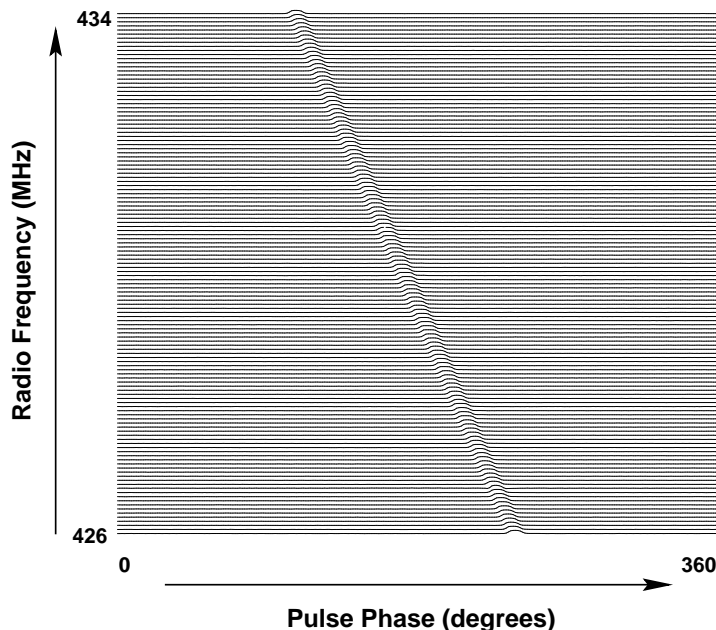


Figure 2. Pulse dispersion shown in this recent 30-s Arecibo observation of PSR B1933+16 across an 8-MHz passband centred at 430 MHz. The period of this pulsar is 358.7 ms. The dispersive time delay between 434 MHz and 426 MHz is 133 ms.

One of the phenomena clearly noted in the discovery paper was pulse dispersion — pulses at higher radio frequencies arrive earlier at the telescope than their lower frequency counterparts. An example of this is shown in Fig. 2. Hewish et al. correctly interpreted the effect as the frequency dependence of group velocity of radio waves as they propagate through the interstellar medium — a cold ionised plasma.

Applying standard plasma physics formulae, it can be shown (see e.g. Lyne & Smith 1998) that the difference in arrival times Δt between a high frequency ν_{hi} (MHz) and a low frequency ν_{lo} (MHz) is given by

$$\Delta t = 4.15 \times 10^6 \text{ ms} \times (\nu_{\text{lo}}^{-2} - \nu_{\text{hi}}^{-2}) \times \text{DM}, \quad (1)$$

where the dispersion measure DM ($\text{cm}^{-3} \text{ pc}$) is the integrated column density of free electrons along the line of sight:

$$\text{DM} = \int_0^d n_e dl. \quad (2)$$

Here, d is the distance to the pulsar (pc) and n_e is the free electron density (cm^{-3}). Pulsars at large distances have higher column densities, and therefore larger DMs, than pulsars closer to Earth so that, from Eq. 1, the dispersive delay across the bandwidth is greater. In the original discovery paper, Hewish et al. (1968) measured a delay for the first pulsar (B1919+21) of $\simeq 0.2$ s between 81.5 and 80.5 MHz. From Eq. 1, we infer a DM of about $13 \text{ cm}^{-3} \text{ pc}$. Assuming, as a first-order approximation, that the mean Galactic electron density is 0.03 cm^{-3} (Ables & Manchester 1976), this implies a distance of about 0.4 kpc ¹.

The most straightforward method to compensate for pulse dispersion is to use a filterbank to sample the passband as a number of contiguous channels and apply successively larger time delays (calculated from Eq. 1)

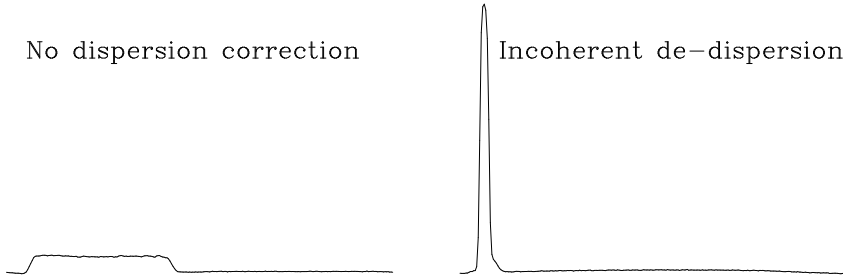


Figure 3. Left: the “raw profile” of B1933+16 formed by the direct addition of individual filterbank channels in Fig. 2. Right: incoherently de-dispersed profile formed by delaying the filterbank channels before addition. Both displays have the same scale.

to higher frequency channels *before* summing over all channels to produce a sharp “de-dispersed” profile. This can be carried out either in hardware or in software. Fig. 3 shows the clear gain in signal-to-noise ratio and time resolution achieved when the data from Fig. 2 are properly de-dispersed, as opposed to a simple detection over the whole bandwidth.

¹Hewish et al. (1968) assumed 0.2 cm^{-3} which resulted in an underestimated distance, but still clearly demonstrated that the source is located well beyond the solar system.

The fact that the free electrons in the Galaxy are finite in extent is well demonstrated by Fig. 4 which shows the dispersion measures of 700 pulsars plotted against the absolute value of their respective Galactic latitudes. It is straightforward to show that, for a simple slab model of free electrons with a mean density n and half-height H , the maximum DM for a given line of sight along a latitude b is $Hn/\sin b$. The solid curve in Fig. 4 shows fairly convincingly that this simple model accounts for the trend rather well implying that $Hn \sim 30 \text{ pc cm}^{-3}$. Taking $n = 0.03 \text{ cm}^{-3}$ as before gives us a first-order estimate of the thickness of the electron layer — about 1 kpc.

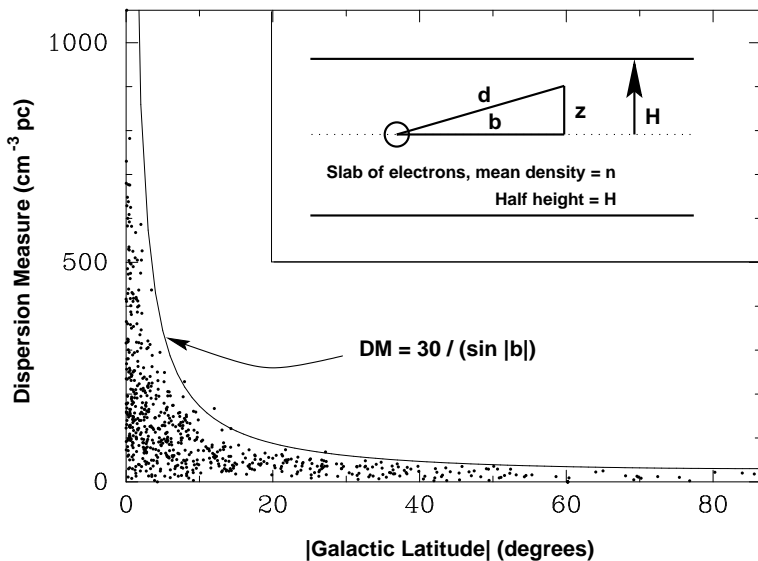


Figure 4. Dispersion measures plotted against Galactic latitudes. Inset: a simple slab model to explain the envelope of points in terms of a finite electron layer (solid curve).

Independent measurements of pulsar distances can, for a large enough sample, be fed back into Eq. 2 to calibrate the Galactic distribution of free electrons. There are three basic distance measurement techniques: neutral hydrogen absorption, trigonometric parallax (measured either with an interferometer or through pulse time-of-arrival techniques) and from associations with objects of known distance (i.e. supernova remnants, globular clusters and the Magellanic Clouds). Together, these provide measurements of (or limits on) the distances to over 100 pulsars. Taylor & Cordes (1993) have used these distances, together with measurements of interstellar scattering for various Galactic and extragalactic sources, to calibrate an electron density model. In a statistical sense, the model can be used to provide distance estimates with an uncertainty of $\sim 30\%$. Although the model is free of large systematic trends, its use to estimate distances to individual pulsars may result in systematic errors by as much as a factor of two.

3. Erratic Individual Pulses and Stable Integrated Profiles

Pulsars are weak radio sources. Mean flux densities, usually quoted in the literature at a radio frequency of 400 MHz, vary between 1 and 100 mJy ($1 \text{ Jy} = 10^{-26} \text{ W m}^{-2} \text{ Hz}^{-1}$). This means that the addition of many thousands of pulses is required in order to produce a discernible profile. Only a handful of sources presently known are strong enough to allow studies of individual pulses. A remarkable fact from these studies is that, although the individual pulses vary quite dramatically, at any particular observing frequency the integrated profile is very stable. This is illustrated in Fig. 5.

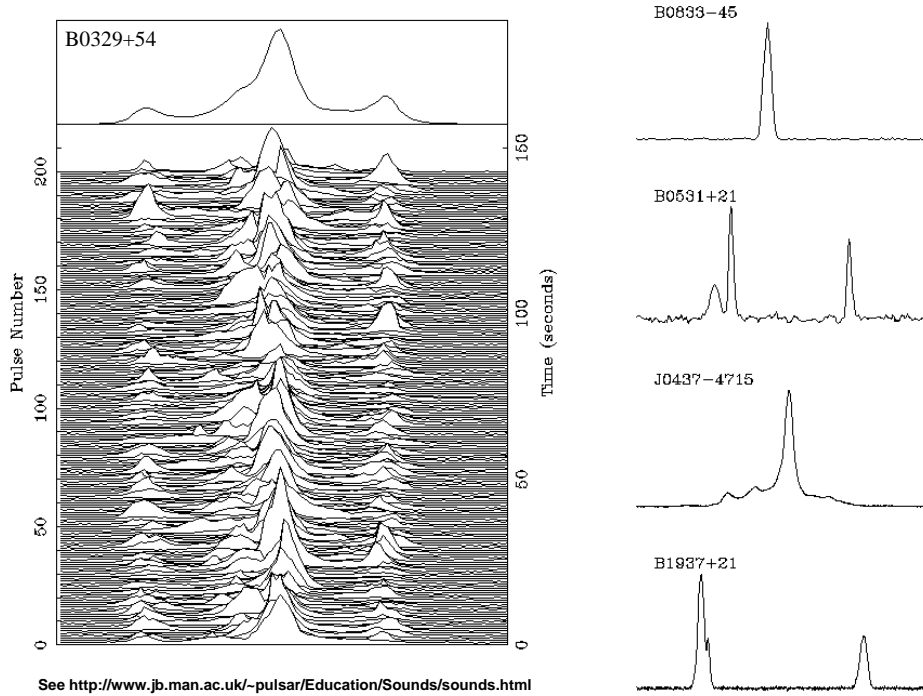


Figure 5. Left: a sequence of 200 individual pulses received from the strong pulsar B0329+54 showing the rich diversity of emission from one pulse to the next. The sum of all the pulses forms a characteristic “integrated profile” shown for this pulsar in the box at the top. Right: some other examples of these stable waveforms.

In the above examples of stable pulse profiles, which have been normalised to represent 360 degrees of rotational phase, the astute reader will notice two examples of so-called interpulses — a secondary pulse separated by about 180 degrees from the main pulse. The most natural interpretation for this phenomenon is that the two pulses originate from opposite magnetic poles of the neutron star (see however Manchester & Lyne 1977).

Geometrically speaking, this is a rather unlikely situation. As a result, the fraction of the known pulsars with interpulses is only a few percent.

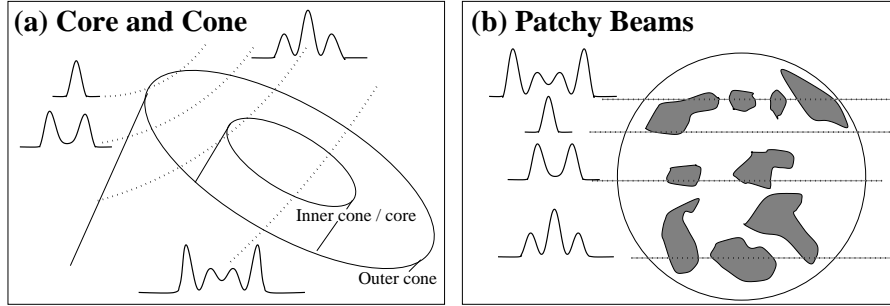


Figure 6. Phenomenological models for pulse shape morphology produced by different line-of-sight cuts of the beam. (Figure designed by M. Kramer and A. von Hoensbroech).

The integrated pulse profile should really be thought of as a unique “fingerprint” of the radio emission beam of each neutron star. The rich variety of pulse shapes can be attributed to different line-of-sight cuts through the radio beam of the neutron star as it sweeps past the Earth. Two contrasting phenomenological models which account for this are shown in Fig. 6. The “core and cone” model, proposed by Rankin (1983), depicts the beam as a core surrounded by a series of nested cones. Alternatively, the “patchy beam” model, championed by Lyne & Manchester (1988), has the beam populated by a series of emission regions.

4. Pulsar Timing Basics

Soon after their discovery, it became clear that pulsars are excellent celestial clocks. Hewish et al. (1968) demonstrated that the period of the first pulsar, B1919+21, was stable to one part in 10^7 over a time-scale of a few months. Following the discovery of the millisecond pulsar, B1937+21, in 1982 (Backer et al. 1982) it was demonstrated that its period could be measured to one part in 10^{13} or better (Davis et al. 1985). This unrivaled stability leads to a host of applications including time keeping, probes of relativistic gravity and natural gravitational wave detectors. Subsequently, a whole science has developed to accurately measure the pulse time-of-arrival in order to extract as much information about each pulsar as possible.

Fig. 7 summarises the essential steps involved in a pulse “time-of-arrival” (TOA) measurement. Incoming pulses emitted by the rotating neutron star traverse the interstellar medium before being received by the radio telescope. After amplification by high sensitivity receivers, the pulses are de-dispersed (§2) and added to form a mean pulse profile. During the observation, the data regularly receive a time stamp, usually based on a maser

at the observatory, plus a signal from the GPS (Global Positioning System of satellites) time system. The TOA of this mean pulse is then defined as the arrival time of some fiducial point on the profile. Since the mean profile has a stable form at any given observing frequency (§3) the TOA can be accurately determined by a simple cross-correlation of the observed profile with a high signal-to-noise “template” profile — obtained from the addition of many observations of the pulsar at a particular observing frequency.

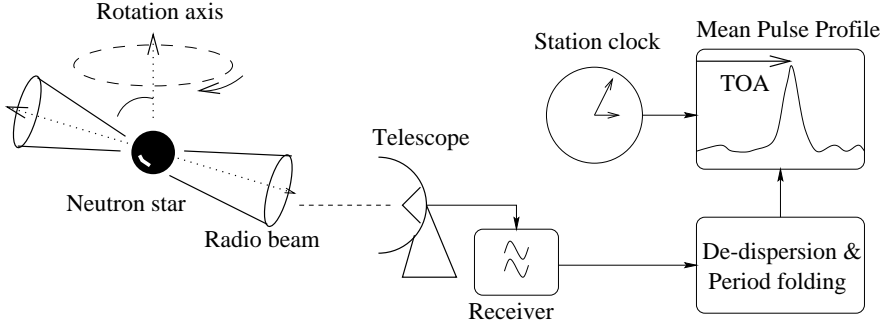


Figure 7. Schematic showing the main stages involved in pulsar timing observations.

In order to properly model the rotational behaviour of the neutron star, we require TOAs as measured by an inertial observer. Due to the Earth’s orbit around the Sun, an observatory located on Earth experiences accelerations with respect to the neutron star. The observatory is therefore not in an inertial frame. To a very good approximation, the centre-of-mass of the solar system, the solar system barycentre, can be regarded as an inertial frame. It is standard practice to transform the observed TOAs to this frame using a planetary ephemeris.

Following the accumulation of about ten to twenty barycentric TOAs from observations spaced over at least several months, a surprisingly simple model can be applied to the TOAs and optimised so that it is sufficient to account for the arrival time of any pulse emitted during the time span of the observations, and predict the arrival times of subsequent pulses. The model is based on a Taylor expansion of the angular rotational frequency about a model value at some reference epoch to calculate a model pulse phase as a function of time. Based upon this simple model, and using initial estimates of the position, dispersion measure and pulse period, a “timing residual” is calculated for each TOA as the difference between the observed and predicted pulse phases (see e.g. Lyne & Smith 1998).

Ideally, the residuals should have a zero mean and be free from any systematic trends (Fig. 8a). Inevitably, however, due to our *a-priori* ignorance of the rotational parameters, the model needs to be refined in a bootstrap fashion. Early sets of residuals will exhibit a number of trends indicating a

systematic error in one or more of the model parameters, or a parameter not initially incorporated into the model. For example, a parabolic trend results from an error in the period time derivative (Fig. 8b). Additional effects will arise if the assumed position of the pulsar used in the barycentric time calculation is incorrect. A position error of just one arcsecond results in an annual sinusoid (Fig. 8c) with a peak-to-peak amplitude of about 5 ms for a pulsar on the ecliptic; this is easily measurable for typical TOA uncertainties of order one milliperiod or better. Similarly, the effect

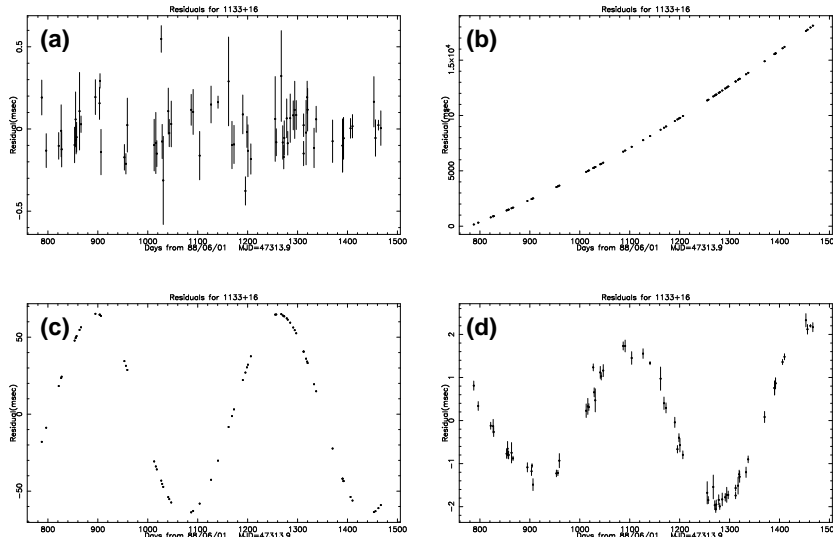


Figure 8. Timing model residuals versus date for PSR B1133+16. Case (a) shows the residuals obtained from the best fitting model which includes period, period derivative, position and proper motion. Case (b) is the result of setting the period derivative term to zero in this model. Case (c) shows the effect of a 1 arcmin error in the assumed declination. Case (d) shows the residuals obtained assuming zero proper motion.

of a proper motion produces an annual sinusoid of linearly increasing magnitude (Fig. 8d). Proper motions are, for many long-period pulsars, more difficult to measure due to the confusing effects of timing noise (a random walk process seen in the timing residuals; see e.g. Cordes & Helfand 1980). For these pulsars, interferometric techniques can be used to obtain proper motions (see Ramachandran’s contribution and references therein).

In summary, a phase-connected timing solution obtained over an interval of a year or more will, for an isolated pulsar, provide an accurate measurement of the period, the rate at which the neutron star is slowing down, and the position of the neutron star. Presently, measurements of these essential parameters are available for about 600 pulsars. The implications of these measurements for the ages and magnetic fields of neutron stars will be discussed in my other contribution to this volume.

For binary pulsars, the model needs to be extended to incorporate the additional radial accelerations of the pulsar as it orbits the common centre-of-mass of the binary system. Treating the binary orbit using just Kepler’s laws to refer the TOAs to the binary barycentre requires five additional model parameters: the orbital period, projected semi-major orbital axis, orbital eccentricity, longitude of periastron and the epoch of periastron passage. The Keplerian description of the orbit is identical to that used for spectroscopic binary stars where a characteristic orbital “velocity curve” shows the radial component of the star’s velocity as a function of time. The analogous plot for pulsars is the apparent pulse period against time. For circular orbits the behaviour is sinusoidal whilst for eccentric orbits the curve has a “saw-tooth” appearance. Two examples are shown in Fig. 9.

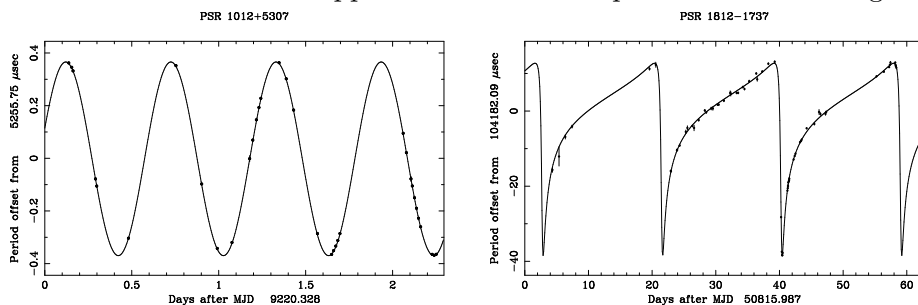


Figure 9. Two different binary pulsars. Left: PSR J1012+5307 — a 5.25-ms pulsar in a 14.5-hour circular orbit around a low-mass white dwarf companion (Nicastro et al. 1995). Right: PSR J1811–1736 (Lyne et al. 2000). A 104-ms pulsar in a highly eccentric 18.8-day orbit around a massive companion (probably another neutron star).

Also by analogy with spectroscopic binaries, constraints on the mass of the orbiting companion can be placed by combining the projected semi-major axis $a_p \sin i$ and the orbital period P_o to obtain the mass function:

$$f(m_p, m_c) = \frac{4\pi^2}{G} \frac{(a_p \sin i)^3}{P_o^2} = \frac{(m_c \sin i)^3}{(m_p + m_c)^2}, \quad (3)$$

where G is the universal gravitational constant. Assuming a pulsar mass m_p of $1.35 M_\odot$ (see below), the mass of the orbiting companion m_c can be estimated as a function of the (initially unknown) angle i between the orbital plane and the plane of the sky. The minimum companion mass m_{\min} occurs when the orbit is assumed edge-on ($i = 90^\circ$).

Further information on the orbital inclination and component masses may be obtained by studying binary systems which exhibit a number of relativistic effects not described by Kepler’s laws. Up to five “post-Keplerian” parameters exist within the framework of general relativity. Three of these parameters (the rate of periastron advance, a gravitational redshift parameter, and the orbital period derivative) have been measured for the original

binary pulsar, B1913+16 (Taylor & Weisberg 1989), allowing high-precision measurements of the masses of both components, as well as stringent tests of general relativity. A further two post-Keplerian parameters related to the Shapiro delay in the double neutron star system PSR B1534+12 have now also been measured (Stairs et al. 1998). Based on these results, and other radio pulsar binary systems, Thorsett & Chakrabarty (1999) have recently demonstrated that the range of neutron star masses has a remarkably narrow underlying Gaussian distribution with a mean of $1.35 M_{\odot}$ and a standard deviation of only $0.04 M_{\odot}$.

5. Pulsar Searching

Pulsar searching is, conceptually at least, a rather simple process — the detection of a dispersed, periodic signal hidden in a noisy time series data taken with a radio telescope. In what follows we give a only brief description of the basic search techniques. Further discussions can be found in Lyne (1988), Nice (1992) and Lorimer (1998) and references therein.

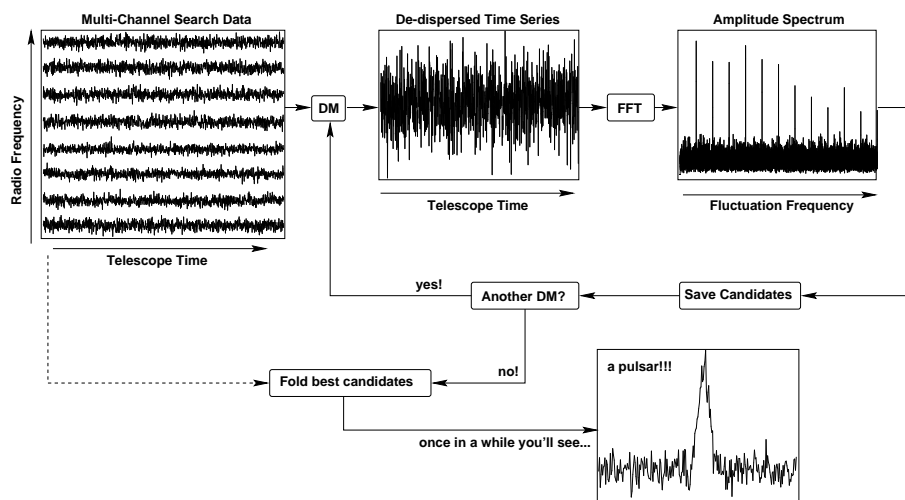


Figure 10. Schematic summarising the essential steps in a “standard” pulsar search.

Most pulsar searches can be pictured as shown in Fig. 10. The multi-channel search data is typically collected using a filterbank or a correlator (see e.g. Backer et al. 1990), either of which usually provides a much finer channelisation than the eight channels shown for illustrative purposes in Fig. 10. The channels are then incoherently de-dispersed (see §2) to form a single noisy time series. An efficient way to find a periodic signal in these data is to take the Fast Fourier Transform (FFT) and plot the resulting amplitude spectrum. For a narrow duty cycle the spectrum will show a

family of harmonics which show clearly above the noise. To detect weaker signals still, a harmonic summing technique is usually implemented at this stage (see e.g. Lyne 1988). The best candidates are then saved and the whole process is repeated for another trial DM.

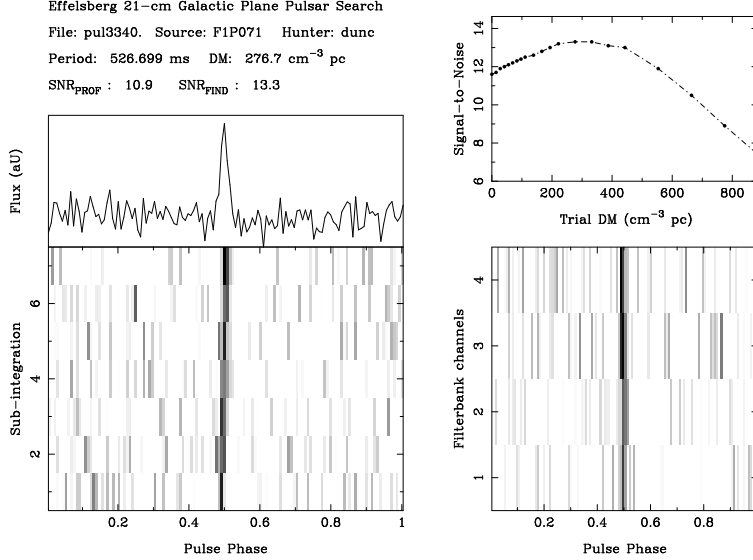


Figure 11. Example search code output showing PSR J1842-0415 — the first pulsar ever discovered with the 100-m Effelsberg radio telescope (Lorimer et al. 2000).

After a sufficiently large number of DMs have been processed, a list of pulsar candidates is compiled and it is then a matter of folding the raw time series data at the candidate period. Fig. 11 is an excellent example of the characteristics of a strong pulsar candidate. The high signal-to-noise integrated profile (top left panel) can be seen as a function of time and radio frequency in the grey scales (lower left and right panels). In addition, the dispersed nature of the signal is immediately evident in the upper right hand panel which shows the signal-to-noise ratio as a function of trial DM. This combination of diagnostics proves extremely useful in differentiating between pulsar candidates and spurious interference.

In the discussion hitherto we have implicitly assumed that the apparent pulse period remains constant throughout the observation. For searches with long integration times (Fig. 11 represents a 35-min observation), this assumption is only valid for solitary pulsars, or those in binary systems where the orbital periods are longer than about a day. For shorter-period binary systems, as noted by Johnston & Kulkarni (1992), the Doppler shifting of the period results in a spreading of the total signal power over a number of frequency bins in the Fourier domain. Thus, a narrow harmonic becomes smeared over several spectral bins.

To quantify this effect, consider the resolution in fluctuation frequency (the width of a Fourier bin) $\Delta f = 1/T$, where T is the length of the integration. It is straightforward to show that the drift in frequency of a signal due to a constant acceleration² a during this time is $aT/(Pc)$, where P is the true period of the pulsar and c is the speed of light. Comparing these two quantities, we note that the signal will drift into more than one spectral bin if $aT^2/(Pc) > 1$. Thus, without due care, long integration times potentially kill off all sensitivity to short-period pulsars in exciting tight orbits where the line-of-sight accelerations are high!

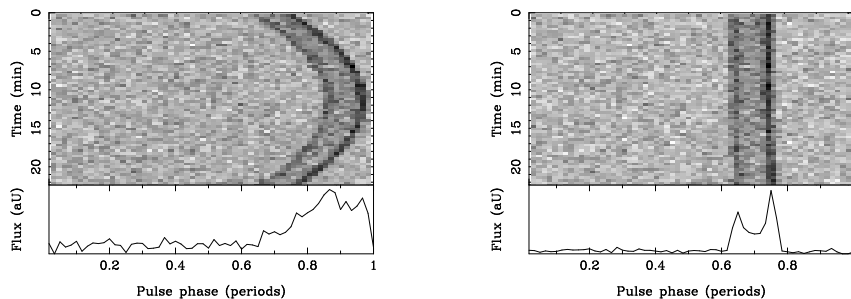


Figure 12. Left: a 22.5-min Arecibo observation of the binary pulsar B1913+16. The assumption that the pulsar has a constant period during this time is clearly inappropriate given the drifting in phase of the pulse during the integration (grey scale plot). Right: the same observation after applying an acceleration search. This shows the effective recovery of the pulse shape and a significant improvement (factor of 7) in the signal-to-noise ratio.

As an example of this effect, as seen in the time domain, Fig. 12 shows a 22.5-min search mode observation of Hulse & Taylor’s binary pulsar B1913+16. Although this observation covers only about 5% of the orbit (7.75 hr), the effects of the Doppler smearing on the pulse signal are very apparent. Whilst the search code nominally detects the pulsar with a signal-to-noise ratio of 9.5 for this observation, it is clear that the Doppler shifting of the pulse period seen in the individual sub-integrations results in a significant reduction in the signal-to-noise ratio.

Pulsar searches of distant globular clusters are most prone to this effect since long integration times are required to reach a reasonable level of sensitivity. Since one of the motivations for searching clusters is their high specific incidence of low-mass X-ray binaries, it is likely that short orbital period pulsars will also be present. Anderson et al. (1990) were the first to really address this problem during their survey of a number of globular clusters using the Arecibo radio telescope. In the so-called acceleration search, the pulsar is assumed to have a constant acceleration (a) during the integration. Each de-dispersed time series can then be re-sampled to

²The smearing is even more severe if a varies — i.e. extremely short orbital periods.

refer it to the frame of an observer with an identical acceleration. This transformation is readily achieved by applying the Doppler formula to relate a time interval in the pulsar frame, τ , to that in the observed frame at time t , as $\tau(t) = \tau_0(1 + at/c)$, where a is the observed radial acceleration of the pulsar along the line-of-sight, c is the speed of light, and τ_0 is a normalising constant (for further details, see Camilo et al. 2000a). If the correct acceleration is chosen, then the net effect is a time series containing a signal with a constant period which can be found using the standard pulsar search outlined above. An example of this is shown in the right panel of Fig. 12 where the time series has been re-sampled assuming a constant acceleration of -17 m s^{-2} . The signal-to-noise ratio is increased to 67!

The true acceleration is, of course, *a-priori* unknown, meaning that a large number of acceleration values must be tried in order to “peak up” on the correct value. Although this necessarily adds an extra dimension to the parameter space searched it can pay handsome dividends, particularly in globular clusters where the dispersion measure is well constrained by pulsars already discovered in the same cluster. Anderson et al. (1990) used this technique to find PSR B2127+11C — a double neutron star binary in M15 which has parameters similar to B1913+16. Camilo et al. (2000a) have recently applied the same technique to 47 Tucanae, a globular cluster previously known to contain 11 millisecond pulsars, to aid the discovery of a further 9 binary millisecond pulsars in the cluster.

The new discoveries in 47 Tucanae include a 3.48-ms pulsar in 96-min orbit around a low-mass companion (Camilo et al. 2000a). Whilst this is presently the shortest orbital period for a radio pulsar binary, the mere existence of this pulsar, as well as the 11-min X-ray binary X1820–303 in the globular cluster NGC6624 (Stella et al. 1987), strongly suggests that there is a population of extremely short-period radio pulsar binaries residing in globular clusters just waiting to be found. As Camilo et al. demonstrate, the assumption of a constant acceleration during the observation clearly breaks down for such short orbital periods, requiring alternative techniques.

One obvious extension is to include a search over the time derivative of the acceleration. This is currently being tried on some of the 47 Tucanae data. Although this does improve the sensitivity to short-period binaries, it is computationally rather costly. An alternative technique developed by Ransom, Cordes & Eikenberry (in prep. see also astro-ph/9911073) looks to be particularly efficient at finding binaries whose orbits are so short that many orbits can take place during an integration. This *phase modulation technique* exploits the fact that the periodic signals from such a binary are modulated by the orbit to create a family of periodic sidebands around the nominal spin period of the pulsar. This technique appears to be extremely promising and is currently being applied to radio and X-ray search data.

6. Recent Survey Highlights — The Parkes Multibeam Survey

No current review on pulsar searching would be complete without summarising the revolution in the field that is presently taking place at the 64-m Parkes radio telescope in New South Wales, Australia. With 13×20 -cm 25-K receivers on the sky, along with $13 \times 2 \times 288$ -MHz filterbanks, the telescope is presently making major contributions in a number of different pulsar search projects. In its main use for a Galactic plane survey (Camilo et al. 2000b), the system achieves a sensitivity of 0.15 mJy in 35 min and covers about one square degree of sky per hour of observing — a standard that is far beyond the present capabilities of any other observatory.

The staggering total of over 500 new pulsars has come from an analysis of about half the total data. Such a large haul is resulting in significant numbers of interesting individual objects: several of the new pulsars are observed to be spinning down at high rates, suggesting that they are young objects with large magnetic fields. The inferred age for the 400-ms pulsar J1119–6127, for example, is only 1.6 kyr. Another member of this group is the 4-s pulsar J1814–1744, an object that may fuel the ever-present “injection” controversy surrounding the initial spin periods of neutron stars (see however my other contribution to these proceedings).

A number of the new discoveries from the survey have orbiting companions. Several low-eccentricity systems are known where the likely companions are white dwarf stars. Two possible double neutron star systems are presently known: J1811–1736 (see Fig. 9), while J1141–65 has a lower eccentricity but an orbital period of only 4.75 hr. The fact that J1141–65 may have a characteristic age of just over 1 Myr implies that the likely birth-rate of such objects may be large. Although tempting, it is premature to extrapolate the properties of one object. It is, however, clear that these binary systems, and the many which will undoubtedly come from this survey, will teach us much about the still poorly-understood population of double neutron star systems (see Kalogera’s contribution in this volume).

The Parkes multibeam system has not only been finding young, distant pulsars along the Galactic plane. Edwards et al. (in prep. see also astro-ph/9911221) have been using the same system to search intermediate Galactic latitudes ($5^\circ \leq |b| \leq 15^\circ$). The discovery of 8 short-period pulsars during this search, not to mention 50 long-period objects, strongly supports a recent suggestion by Toscano et al. (1998) that L-band (λ 20 cm) searches are an excellent means of finding relatively distant millisecond pulsars.

The most massive binary system yet from either of these two multibeam surveys is J1740–3052, whose orbiting companion must be at least $11 M_\odot$! Recent optical observations (Manchester et al. 2000) reveal a K-supergiant as being the likely companion star in this system. With such high-mass

systems in the Galaxy, surely it is only a matter of time before a radio pulsar will be found orbiting a stellar-mass black hole.

Having finally made the connection between neutron stars and black holes, I will finish by reiterating that pulsar astronomy is currently enjoying one of the most productive phases in its history. The new discoveries are sparking off a variety of follow-up studies of all the exciting new objects. There will surely be plenty of surprises in the coming years and new students are encouraged to join this hive of activity.

Acknowledgements

Many thanks to Chris Salter and Fernando Camilo for their comments on an earlier version of this manuscript. The Arecibo Observatory is operated by Cornell University under a cooperative agreement with the NSF.

References

- Ables J. G., Manchester R. N., 1976, *A&A*, 50, 177
 Anderson S. B. et al. 1990, *Nat*, 346, 42
 Baade W., Zwicky F., 1934, *Proc. Nat. Acad. Sci.*, 20, 254
 Backer D. C. et al. 1982, *Nat*, 300, 615
 Backer D. C., Clifton T. R., Kulkarni S. R., Wertheimer D. J., 1990, *A&A*, 232, 292
 Camilo F. et al. 2000a, *ApJ*, in press, (astro-ph/9911234)
 Camilo F. et al. 2000b, *Pulsar Astronomy — 2000 and Beyond*, (astro-ph/9911185)
 Cordes J. M., Helfand D. J., 1980, *ApJ*, 239, 640
 Davis M. M., Taylor J. H., Weisberg J. M., Backer D. C., 1985, *Nat*, 315, 547
 Gold T., 1968, *Nat*, 218, 731
 Hewish A., Bell S. J., Pilkington J. D. H., Scott P. F., Collins R. A., 1968, *Nat*, 217, 709
 Hulse R. A., Taylor J. H., 1975, *ApJ*, 195, L51
 Johnston H. M., Kulkarni S. R., 1992, *ApJ*, 393, L17
 Lorimer D. R., 1998, in Davier M., Hello P., Eds, *Second Workshop on Gravitational Wave Data Analysis*. Editions Frontiers, p. 121 (astro-ph/9801091)
 Lorimer D. R. et al. 2000, *A&A*, submitted, (astro-ph/9910569)
 Lyne A. G., Manchester R. N., 1988, *MNRAS*, 234, 477
 Lyne A. G., Smith F. G., 1998, *Pulsar Astronomy*. Cambridge University Press
 Lyne A. G., 1988, in Schutz B., Ed, *Gravitational Wave Data Analysis*, Dordrecht, p. 95
 Lyne A. G. et al. 2000, *MNRAS*, in press (astro-ph/9911313)
 Manchester R. N., Lyne A. G., 1977, *MNRAS*, 181, 761
 Manchester R. N. et al. 2000, *Pulsar Astronomy — 2000 and Beyond*, (astro-ph/9911319)
 Nicastro L. et al. 1995, *MNRAS*, 273, L68
 Nice D. J., 1992, PhD thesis, Princeton University
 Pacini F., 1968, *Nat*, 219, 145
 Rankin J. M., 1983, *ApJ*, 274, 333
 Stairs I. H. et al. 1998, *ApJ*, 505, 352
 Stella L., Priedhorsky W., White N. E., 1987, *ApJ*, 312, L17
 Taylor J. H., Cordes J. M., 1993, *ApJ*, 411, 674
 Taylor J. H., Weisberg J. M., 1989, *ApJ*, 345, 434
 Thorsett S. E., Chakrabarty D., 1999, *ApJ*, 512, 288
 Toscano M., Bailes M., Manchester R. N., Sandhu J., 1998, *ApJ*, 506, 863
 Wolszczan A., Frail D. A., 1992, *Nat*, 355, 145